A repulsive skyrmion chain as a guiding track for a racetrack memory (F)

D. Suess, C. Vogler, F. Bruckner, P. Heistracher (iD), and C. Abert

COLLECTIONS

(F) This paper was selected as Featured

View Online   Export Citation   CrossMark

ARTICLES YOU MAY BE INTERESTED IN

The design and verification of MuMax3
AIP Advances **4**, 107133 (2014); https://doi.org/10.1063/1.4899186
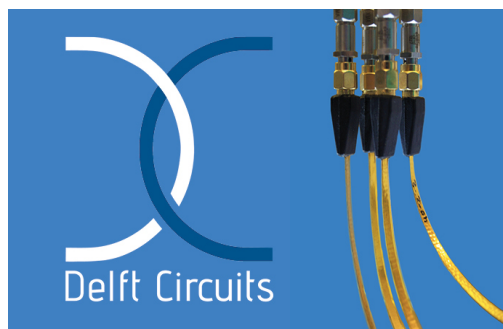
Perspective: Magnetic skyrmions—Overview of recent progress in an active research field
Journal of Applied Physics **124**, 240901 (2018); https://doi.org/10.1063/1.5048972

Origin of Na causing potential-induced degradation for p-type crystalline Si photovoltaic modules
AIP Advances **8**, 115311 (2018); https://doi.org/10.1063/1.5040516

A repulsive skyrmion chain as a guiding track for a racetrack memory

D. Suess,[1,a] C. Vogler,[2] F. Bruckner,[1] P. Heistracher,[1] and C. Abert[1]
[1]*Doppler Laboratory "Advanced Magnetic Sensing and Materials," University of Vienna, Währinger Straße 17, 1090 Vienna, Austria*
[2]*Physics of Functional Materials, University of Vienna, Währinger Straße 17, 1090 Vienna, Austria*

A skyrmion racetrack design is proposed that allows for thermally stable skyrmions to code information and dynamical pinning sites that move with the applied current. This concept solves the problem of intrinsic distributions of pinning times and pinning currents of skyrmions at static pinning sites due to geometrical constrictions or disordered film. The dynamical pinning sites are realized by a skyrmion carrying wire, where the skyrmion repulsion is used in order to keep the skyrmions at equal distances. The information is coded by an additional layer where the presence and absence of a skyrmion is used to code the information. The lowest energy barrier for a data loss is calculated to be $\Delta E = 55$ $k_B T_{300}$ which is sufficient for a long time thermal stability. © 2018 Author(s). *All article content, except where otherwise noted, is licensed under a Creative Commons Attribution (CC BY) license (http://creativecommons.org/licenses/by/4.0/).* https://doi.org/10.1063/1.4993957

Skyrmion racetrack devices that store information by the presence or absence of skyrmions have recently attracted significant attention.[1–4] Extensive research has been performed in order to calculate the stability of individual skyrmions for infinitely extended magnetic structures. Using variants of the nudged elastic band method,[5] that is a well established tool for magnetic structures,[6] the energy barrier for skyrmion annihilation via Bloch point like singularities was studied recently.[7–12] Good agreement between different string like methods such as the geodesic nudged elastic band[7,13] and the string method[14] could be found for isotropic collapse.[12] In addition, the stability of skyrmions has also estimated by Langevin simulations.[8] In contrast to Bloch points that occur for example during the reversal of a vortex core and the position of the Bloch point varies along the perpendicular direction, in the case of skyrmions we refer to a Bloch point-like singularity (in the following we name it Bloch point) any singular, where the corresponding energy increases with decreasing mesh size in a micromagnetic simulations. This singularity may also arise within a plane. Skyrmions are usually considered to be topological protected, whereas there is scientific debate whether topological protection in continuous system means, that the change of the topological charge requires an infinite energy barrier[15] or a finite barrier.[16,17] If a finite energy barrier is still regarded as topological protected even annihilation of a skyrmion via the boundary, which has usually the smallest energy barrier and does not form a Bloch point[3,14,18,19] will be regarded as topological protected, even so the stabilities might be in the nanosecond regimes.

The stability of skyrmions against annihilation is often considered to be the most important feature for storage applications. However, this kind of stability is not a sufficient condition for stable data. Since in skyrmion racetrack memory the information is coded by the distance between skyrmions it has to be guaranteed that (i) the position (distance) of the skyrmion is thermally stable and (ii) if a current pulse is applied in a skyrmion racetrack shift register the distance between all the skyrmions remain the same. Whereas requirement (i) can be realized by pinning sites that can be constructed by geometrical or magnetic features,[18] requirement (ii) is not solved with the original racetrack concept.

[a]Correspondence to dieter.suess@univie.ac.at

Finite temperature and distributions in the pinning sites lead to a distribution in depinning currents, times[18] and velocities[20] that are expected to lead to read and write error rates that are significantly too large for practical applications.[18] If for example a too short current pulse is applied, the skyrmion may not move over the pinning site. If a too long current pulse is applied, the skyrmion may move over two pinning sites.

For comparison, the required write error rates in random access memory must be smaller than 10^{-9} as reviewed in Ref. 21. In hard disk storage a lower BER can be tolerated since the error correction is applied to all bits within a sectors which makes ECC more efficient compared to random access memory (RAM). This extensive error correction in hard disk reduce the overall unrecoverable bit error rate to 10^{-16} - 10^{-14}.[22]

In order to achieve BER $< 10^{-9}$ in skyrmion devices with predefined pinning sites to locate the bits (skyrmions) at well-defined positions, the depinning time distribution divided by the mean traveling time of the skyrmion from one pinning site to the next pinning site must be smaller than about 5%.[18] For comparison, the switching time distribution divided by the mean switching time in MRAM cells is measured to be around 30%.[23]

Alternatively, one might aim to use wires without special predesigned pinning sites and might rely on natural pinning sites of the wire due to the disorder of the film.[20] Here, an equivalent problem as mentioned above occurs. After the application of a current pulse, all skyrmions in the wire do not move exactly the same distance due to disorder in the film[20] and finite temperature. As a consequence, the information that is coded by the distance between the skyrmions might be lost. In order to be able to read out data with an error rate smaller than 10^{-9} the distance of the skyrmions has to be larger than $d = 413$ nm as approximated in Ref. 18 for a particular system. This is a linear density worse by a factor of about 40 compared to conventional hard disks.

In this work, we present a concept that solves the before mentioned problems. The concept utilizes two magnetic layers, which are separated by a non-magnetic layer as shown in Fig. 1. In order to realize stable skyrmions, each layer within this study consists of $[Pt/Co/Ta]_n$ multilayers, where n is the number of repetitions.[24] The bottom layer does not store information but it is used to realize moveable pinning sites in the form of skyrmions. The repulsion of skyrmions[25] is used in order to keep the distance of these skyrmions approximately constant. The information is coded in the top layer by the presence (bit 1) or absence (bit 0) of skyrmions that are coupled via strayfield interaction to a position above the skyrmions in the bottom layer. The fundamental difference and advantage of the presented concept compared to conventional racetrack concepts is that due to the repulsion of the skyrmions in the bottom layer a mechanism exists that restores the original distances between the skyrmions in the top layer.

On the left-hand side of the wire, skyrmions are created in the top layer according to the information that should be written, for example by means of spin transfer torque.[1] This information is moved by applying a current within both layers in the direction indicated by the arrow in Fig. 1. Due
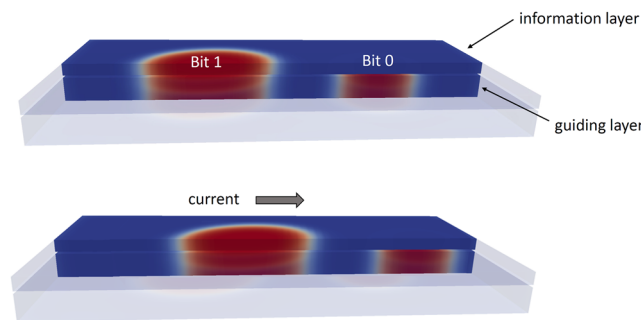

FIG. 1. Schematic view of the working principle of the gap protecting skyrmion device. The structure consists of two exchange decoupled layers. The top layer (information layer) stores the information by the presence and absence of a skyrmion. In order to keep the distance between these states, they are coupled via strayfield interaction to the bottom layer (guiding layer). This layer contains skyrmions at each bit position that are kept constant in distance due to their repulsive force. For writing and reading current pulses are applied until the bottom skyrmions move by one bit position.

to the current, spin transfer torque due to magnetization inhomogeneity within the Co layer arise that can move the skyrmions. In addition, if a current is applied within the two layers due to the current in the heavy metal layers (Pt,Ta) also spin-orbit torque (SOT) may act on the Co layer.[1] However, due to the large spin diffusion length in Pt and Co that are reported to be 14 nm and >40 nm,[26] respectively, SOT that arises within a heavy metal layer does not only act on the adjacent Co but will diffuse and act on several Co layers. Hence, it is expected that the SOT gets partly compensated due to the multilayer structure. The relative strength of these two different spin torque effects will be work of future studies.

On the right-hand side of the layer, the information is read out, for example by means of detecting the strayfield of the skyrmion in the bottom layer and top layer by a TMR sensor. The presence of the skyrmions in the guiding layer can be used as a clock cycle, i.e. whenever a skyrmion is detected in the guiding layer, the magnetic state in the information layer is determined in order to resolve the bit. The problem, that the distance between the skyrmions may change in standard racetrack devices can be overcome with this device. Even if the distance between two skyrmions in one of the layers is changed due to defects, the guiding layer will restore the original distances, which in turn readjusts the skyrmion distance in the information layer. This is in contrast to the original design of racetrack structures where an unintended change of distance cannot be restored again. Compared to the interesting concept of Ref. 27 it is expected that due to the planar magnetic structure the suggested device is significantly easier to fabricate. Furthermore, the data density is expected to be larger by a factor of two.

In the following, we calculate the thermal stability of the stored information by calculating energy barriers between the encoded bit state and various paths towards bit annihilation. For the presented concept it is essential that the skyrmion that is created in the top layer (representing bit 1) stays above the skyrmion in the bottom layer during operation. The field that supports this requirement is the strayfield of the bottom skyrmion that favors skyrmion positions above each other.

For the micromagnetic simulations, a hybrid FEM/BEM method is used.[28] If not stated otherwise, the used mesh size is 3 nm. For the calculation of the energy barrier, the string method is used.[29] In order to redistribute the images along the string we use for the reaction coordinate s_i for the image i,

$$s_0 = 0, \quad s_i = s_{i-1} + W_{i-1/2}|\mathbf{u}_i - \mathbf{u}_{i-1}| \tag{1}$$

Here, $\boldsymbol{u}_i$ contains the $3N$ Cartesian coordinates of the normalized magnetization, the used norm is the L_2 norm and

$$W_{i-1/2} = \left[\left(\frac{E_i + E_{i-1}}{2} - E_{min}\right)/(E_{max} - E_{min}) + 1\right]^{\omega}, \tag{2}$$

where E_i is the total energy of image i and E_{max} and E_{min} the maximum and minimum energy of the list of images, respectively. After 5ps of integrating the Landau-Lifshitz equation without precession term, the images are redistributed by a quadratic spline interpolation, in order to obtain equal distance according to the reaction coordinate defined in Eq. (1). If not stated explicitly $\omega = 0$, which simplifies the distance between the images to the L_2 distance.

The magnetic parameters of the investigated structure are motivated by recent studies of Co layers between heavy metal layer. In Ref. 24 [Pt(3 nm)/Co(0.9 nm)/Ta(4 nm)]$_{15}$ multilayers are studies and the following material parameters are reported: anisotropy constant $K_1 = 0.37$ MJ/m^3, easy axis perpendicular to the film (z-axis), saturation polarization $J_s = 0.75$ T, exchange constant A = 10 pJ/m and the DMI constant is $D = 1.5 \times 10^{-3}$ J/m^2. In Ref. 30 (Ir1|Co0.6|Pt1)$_{10}$|Pt$_3$ structures are studied and the following material parameters are used: $K_1 = 0.72$ MJ/m^3, $J_s = 1.2$ T, A = 10 pJ/m, $D = 1.9 \times 10^{-3}$ J/m^2. In Ref. 31 $K_1 = 0.8$ MJ/m^3, $J_s = 0.72$ T, A = 15 pJ/m, $D = 3.0 \times 10^{-3}$ J/m^2 are assumed.

Within this paper we use parameters for the Co layer that are within the range of Ref. 24,30,31: $K_1 = 0.6$ MJ/m^3, $J_s = 0.72$ T, A = 15 pJ/m and an effective interface exchange within the Co layer of $D = 3 \times 10^{-3}$ J/m^2. We assume a Co layer thickness of 0.5 nm. For the simulations, we do not resolve the multilayer stack but only simulate the Co layers that are directly stacked over each other. This approach is well justified as reported in Ref. 30. Concerning the strayfield interaction between the

bottom and top wire, this approach is an approximation that would be accurate in the limit of infinite thin heavy metal layers.

In order to take into account the interface DMI the additional energy contribution is added to the total energy E_{tot},[32]

$$E_{DMI} = \int D[\mathbf{m} \cdot \nabla m_n - m_n \nabla \mathbf{m}]dV \tag{3}$$

where $m_n = \mathbf{m} \cdot \mathbf{e}_z$ and $\mathbf{e}_z$ is the normal vector of the interfaces.

In the following, we aim to calculate all energy barriers and possible MEP that lead to data loss due to the annihilation or change of position of the skyrmion in the top layer.

In Fig. 2 the energy barrier for a path is calculated, where the skyrmion moves from one pinning site to the next one, as shown by the magnetic states in Fig. 2 (A) and Fig. 2 (D). Here, the z-component of the magnetization is color coded. Red represents magnetization up, blue represents magnetization down. The thickness of the guiding layer and the information layer is $t_{bottom} = 10$ nm and $t_{top} = 5$ nm, respectively. These two layers are separated by a 1 nm non-magnetic layer. The lateral dimensions are 180 nm x 90 nm. The energy barrier obtained by the string method is $\Delta E = 55$ $k_B T_{300}$. The saddle point configuration is shown in Fig. 2 (B), where the skyrmion in the information layer partly overlaps with the second skyrmion in the gap protection layer. Interestingly during the motion of the skyrmion of the stable configuration Fig. 2 (A) to Fig. 2 (D) there exists also a local minimum as shown in Fig. 2 (C), where the skyrmion in the top layer increases in size and it is pinned by the stayfield of the two skyrmions in the bottom layers. The energy barrier to leave the stable states (Fig. 2 (A) and Fig. 2 (D)) is sufficiently high to guarantee thermal stability at room temperature.

Another path that leads to data loss is shown in Fig. 3. Here, the energy barrier of the annihilation of the skyrmion in the information layer is calculated. As initial states for the string method two states are chosen. The first state contains the skyrmion in the information layer and the two skyrmions in the gap protection layer (Fig. 3. (A)). The final state contains the same skyrmions in the gap protection layer but no skyrmion in the information layer (Fig. 3. (E)). Hence, here we calculate the energy barrier for the isotropic collapse in the top layer. Interestingly the skyrmion is transformed to an elliptical structure (Fig. 3. (B) - Fig. 3. (C)). The state with maximum energy along the MEP is shown in Fig. 3. (D), where the elliptical structure still has a finite size. Finally, A Bloch point is formed that has however for the used mesh size smaller energy than the state shown in Fig. 3. (D). Due to the formation of a Bloch point, the micromagnetic approach is not valid any longer and it is expected that the results depend on the mesh size.

In order to study the mesh-size dependence of the annihilation process the model is simplified to only one magnetic layer with the dimensions of 90 nm x 90 nm x 0.6 nm, as shown in Fig. 4.
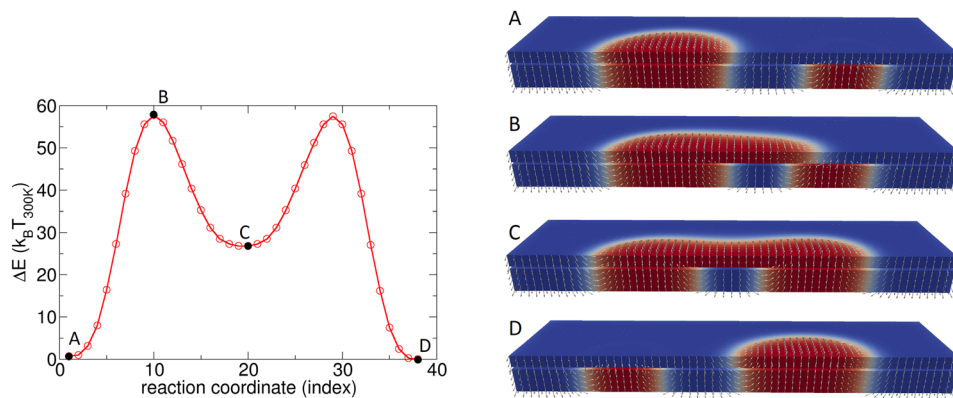

FIG. 2. Energy barrier of bit error process, where the stored information moves to the next dynamical pinning site. The thickness of the guiding layer is $t_{bottum} = 10$ nm and the information layer $t_{top} = 5$ nm. These two layers are separated by a 1 nm non-magnetic layer. The lateral dimensions are 180 nm x 90 nm.
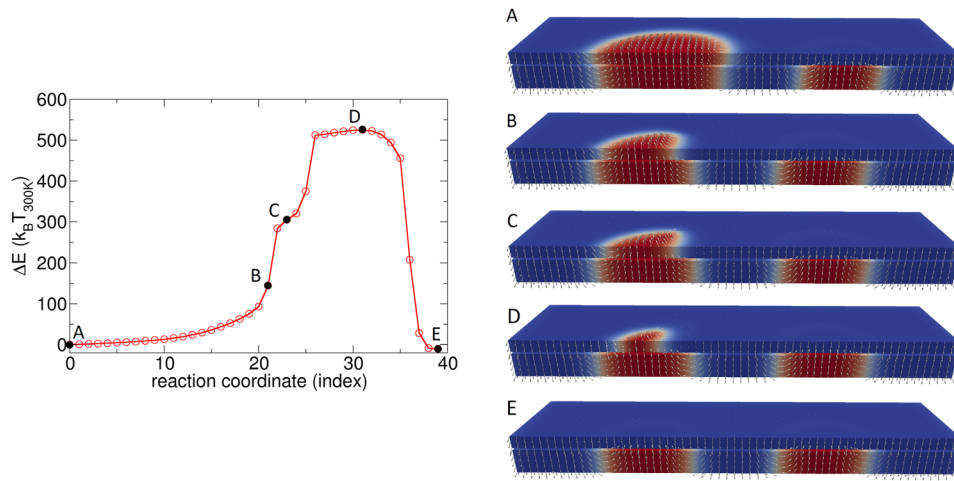
FIG. 3. Energy barrier of bit error process, where the skyrmion in the information layer is annihilated via the formation of a Bloch point.

For this simplified model without the gap protection layer, the MEP is calculated. Fig. 4. shows the magnetic states for a mesh size of 1.6 nm. With increasing reaction coordinate along the minimum energy path the skyrmion diameter decreases in size as shown in Fig. 4 (A-B) until at the saddle point configuration a Bloch point is formed in Fig. 4 (C). A detailed view of the magnetization state is shown in Fig. 4 (C – detailed view). Here, the finite element mesh is shown, where the magnetization is represented by vectors on the node points. At the saddle point four spins are pointing towards each
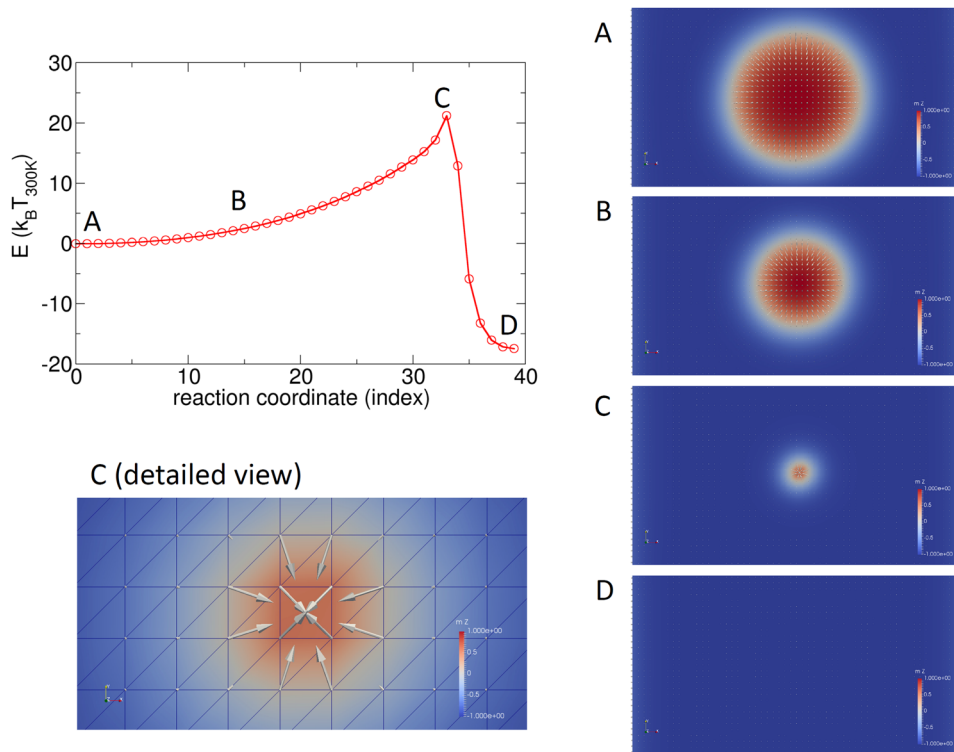

FIG. 4. Detailed calculation of the annihilation of a single skyrmion via the formation of a Bloch point. Only one magnetic layer with a thickness $t = 0.6$ nm is simulated. The lateral dimensions are 90 nm x 90 nm. The discretization mesh size is 1.6 nm.

other significantly contributing to the saddle point energy. This configuration which is obtained with the finite element method using a regular mesh is very similar to the state that is found by an atomistic simulation.[7]

The saddle point energy and the energy barrier depends on the mesh size since the exchange energy of the finite element that contains the Bloch point is determined by the discretization size. Fig. 5 (red circles) shows the energy barrier for annihilation via the described process as a function of mesh size. An almost linear increase of energy barrier with the mesh size can be observed for isotropic annihilation. If the mesh size is chosen similar to the atomistic lattice constant of $a = 0.5$ nm the energy of annihilation via the Bloch point is about a factor 3.2 higher than the energy barrier via annihilation via the boundary.

Since, for the isotropic annihilation via a Bloch point the micromagnetic prerequisite of a continuous magnetization as function of space is not fulfilled we also performed atomistic simulations using 3D Heisenberg spins as described in Ref. 12,14. For the simulation of one layer of Co atoms, where the atomistic parameters are extracted from the micromagnetic parameters with a lattice parameter of $a = 0.5$ nm, we obtain for the isotropic annihilation via a Bloch point $\Delta E = 30\,k_B T_{300}$. This surprisingly well follows the trend of the energy barrier of the finite element method. As described in Ref. 18 the energy barrier linearly increases with the film thickness. Hence, for a 10 nm thick Co-film isotropic annihilation is not the most probably annihilation path of the skymrion for this system.

For boundary annihilation we obtain from the atomistic simulations $\Delta E = 6.6\,k_B T_{300}$ which agrees quite well with the boundary annihilation data obtained from the finite element approach that is, $\Delta E = 7.8\,k_B T_{300}$. Here, it has to be noted that in the atomistic approach the discrete magnetic moments are located on each lattice site, whereas in the micromagnetic simulations a continuous magnetization is assumed. This different discretization results in 7% difference in the shape anisotropy of an infinite film.[33] If the micromagnetic data is extrapolated to a 10 nm thick Co-film the energy barrier can be approximated to be $\Delta E \sim 130\,k_B T_{300}$.

Finally, the reversal path for the annihilation of three skyrmions is calculated as shown in Fig. 6. With the standard parameter of the string method with $\omega = 0$ the energy drastically increases in the vicinity of the saddle point. As a consequence, the saddle point configuration cannot be properly resolved and the simulation does not converge. In order to overcome this problem, the density of images is scaled with an energy norm using $\omega = 10$. It can be seen that this approach is successful and the states around the saddle point can be resolved well. The saddle point configuration is a state where the two skyrmions in the bottom layer start to merge Fig. 6 (C). Since even in this annihilation process the topological charge changes, the formation of a Bloch point occurs. Hence, the micromagnetic simulation is not used to provide the detailed energy barrier but it is used in order to provide a lower limit of the energy barrier since the chosen mesh size is significantly larger than the lattice constant. Since the obtained energy barrier of this annihilation processes is $\Delta E = 445\,k_B T_{300}$ and significantly larger than the annihilation via the boundary this estimate is sufficient to conclude that this annihilation process is not the most critical one.
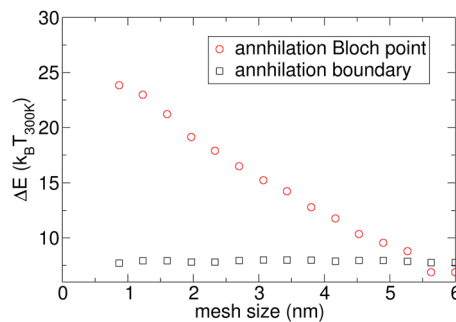

FIG. 5. Mesh size dependence of two annihilation processes of a skyrmion. (red circles) Annihilation within the structure occurs via formation of a Bloch point as shown in Fig. 4. The energy of the Bloch point depends on the discretization. (black squares) annihilation of the skyrmion via the boundary. The energy barrier does not depend on the mesh size, since no Bloch point is formed.
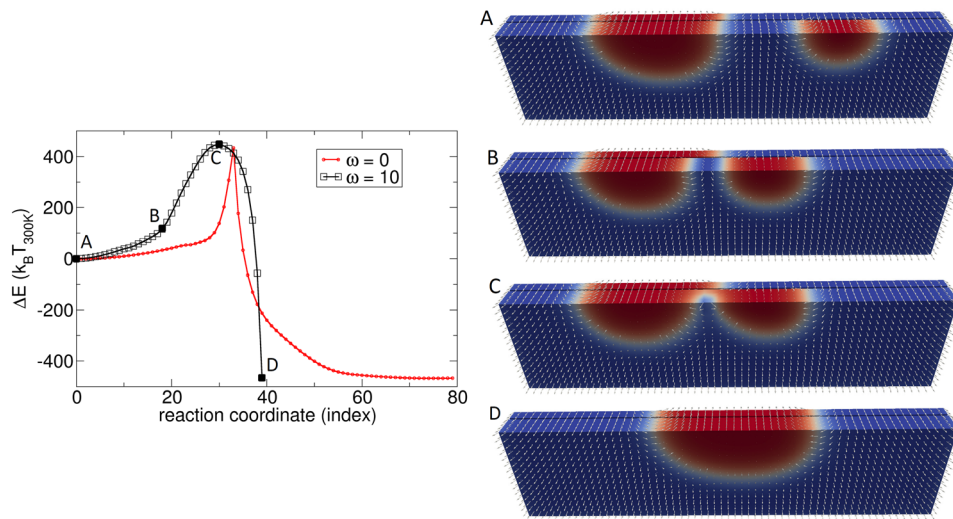
FIG. 6. Energy barrier of bit error process, where three skyrmions are annihilated to two skyrmions. In order to increase the density of the images besides the standard parameter $\omega = 0$ (red), a simulation with $\omega = 10$ is performed (black).

To conclude a concept is proposed that shows how information can be reliably stored in two wires containing skyrmions. The bottom wire is used to generate dynamically moving pinning sites. These pinning sites are used to store the information by the skyrmion positions in the top layer at well-defined distances. Due to the repulsive forces of the skyrmions in the bottom layer, all skyrmions in the shift register will move with a constant distance between them. It is shown that the energy barrier for the annihilation of skyrmions is larger than $\Delta E = 55$ $k_B T_{300}$. This concept solves the significant problem of distributions of pinning times and currents that are a significant error source in skyrmion race track devices.[18] The areal density of the presented structure is 0.04 Tbit/inch^2, which is significantly smaller than the areal density of state-of-the-art magnetic hard disks (1.4 Tbit/inch^2[34]) or FLASH storage. However, skyrmions might be an interesting option for application where the size of the bit is not the leading objective and multiple bits per cell in RAM like devices lead to an increased performance.[35]

[1] A. Fert, V. Cros, and J. Sampaio, "Skyrmions on the track," Nat. Nanotechnol. **8**(3), 152–156 (2013).

[2] R. Tomasello, E. Martinez, R. Zivieri, L. Torres, M. Carpentieri, and G. Finocchio, "A strategy for the design of skyrmion racetrack memories," Sci. Rep. **4**, 6784 (2014).

[3] D. Cortés-Ortuño *et al.*, "Thermal stability and topological protection of skyrmions in nanotracks," ArXiv161107079 Cond-Mat, Nov. 2016.

[4] J. Sampaio, V. Cros, S. Rohart, A. Thiaville, and A. Fert, "Nucleation, stability and current-induced motion of isolated magnetic skyrmions in nanostructures," Nat. Nanotechnol. **8**(11), 839–844 (2013).

[5] G. Henkelman, B. P. Uberuaga, and H. Jónsson, "A climbing image nudged elastic band method for finding saddle points and minimum energy paths," J. Chem. Phys. **113**(22), 9901–9904 (2000).

[6] R. Dittrich, T. Schrefl, D. Suess, W. Scholz, H. Forster, and J. Fidler, "A path method for finding energy barriers and minimum energy paths in complex micromagnetic systems," J. Magn. Magn. Mater. **250**(1–3), L12–L19 (2002).

[7] P. F. Bessarab, V. M. Uzdin, and H. Jónsson, "Method for finding mechanism and activation energy of magnetic transitions, applied to skyrmion and antivortex annihilation," Comput. Phys. Commun. **196**, 335–347 (2015).

[8] S. Rohart, J. Miltat, and A. Thiaville, "Path to collapse for an isolated Néel skyrmion," Phys. Rev. B **93**(21), 214412 (2016).

[9] I. S. Lobanov, H. Jónsson, and V. M. Uzdin, "Mechanism and activation energy of magnetic skyrmion annihilation obtained from minimum energy path calculations," Phys. Rev. B **94**(17), 174418 (2016).

[10] D. Cortés-Ortuño *et al.*, "Thermal stability and topological protection of skyrmions in nanotracks," Sci. Rep. **7**(1), 4060 (2017).

[11] D. Stosic, J. Mulkers, B. Van Waeyenberge, T. B. Ludermir, and M. V. Milošević, "Paths to collapse for isolated skyrmions in few-monolayer ferromagnetic films," Phys. Rev. B, **95**(21) (2017).

[12] P. T. Heistracher, Master Thesis, *Atomistic spin dynamics*, http://repositum.tuwien.ac.at/obvutwhs/content/titleinfo/2281383. Wien: Wien, 2017.

[13] L. Desplat, D. Suess, J.-V. Kim, and R. L. Stamps, "Thermal stability of metastable magnetic skyrmions: Entropic narrowing and significance of internal eigenmodes," ArXiv180206744 Cond-Mat, Feb. 2018.

[14] P. Heistracher, C. Abert, F. Bruckner, C. Vogler, and D. Suess, "GPU-accelerated atomistic energy barrier calculations of skyrmion annihilations," IEEE Trans. Magn., 1–5 (2018).

[15] H.-B. Braun, "Topological effects in nanomagnetism: From superparamagnetism to chiral quantum solitons," Adv. Phys. **61**(1), 1–116 (2012).

[16] F. Büttner, I. Lemesh, and G. S. D. Beach, "Full phase diagram of isolated skyrmions in a ferromagnet," ArXiv170408489 Cond-Mat, Apr. 2017.

[17] A. O. Leonov, T. L. Monchesky, N. Romming, A. Kubetzka, A. N. Bogdanov, and R. Wiesendanger, "The properties of isolated chiral skyrmions in thin magnetic films," New J. Phys. **18**(6), 065003 (2016).

[18] D. Suess, C. Vogler, F. Bruckner, and C. Abert, "Spin torque efficiency and analytic error rate estimates of skyrmion racetrack memory," ArXiv170408164 Cond-Mat, Apr. 2017.

[19] D. Stosic, J. Mulkers, B. Van Waeyenberge, T. Ludermir, and M. V. Milošević, "Paths to collapse for isolated skyrmions in few-monolayer ferromagnetic films," ArXiv170408025 Cond-Mat, Apr. 2017.

[20] J.-V. Kim and M.-W. Yoo, "Current-driven skyrmion dynamics in disordered films," Appl. Phys. Lett. **110**(13), 132404 (2017).

[21] D. Apalkov, B. Dieny, and J. M. Slaughter, "Magnetoresistive random access memory," Proc. IEEE **104**(10), 1796–1830 (2016).

[22] T. R. Albrecht *et al.*, "Bit-patterned magnetic recording: Theory, media fabrication, and recording performance," IEEE Trans. Magn. **51**(5), 1–42 (2015).

[23] Y. Zhang, X. Wang, and Y. Chen, "STT-RAM Cell Design Optimization for Persistent and Non-persistent Error Rate Reduction: A Statistical Design View," in Proceedings of the International Conference on Computer-Aided Design, Piscataway, NJ, USA, 2011, S. 471–477.

[24] S. Woo *et al.*, "Observation of room-temperature magnetic skyrmions and their current-driven dynamics in ultrathin metallic ferromagnets," Nat. Mater. **15**(5), 501–506 (2016).

[25] X. Zhang *et al.*, "Skyrmion-skyrmion and skyrmion-edge repulsions in skyrmion-based racetrack memory," Sci. Rep. **5**, srep07643 (2015).

[26] J. Bass and W. P. Pratt, Jr., "Spin-diffusion lengths in metals and alloys, and spin-flipping at metal/metal interfaces: an experimentalist's critical review," J. Phys. Condens. Matter **19**(18), 183201 (2007).

[27] J. Müller, "Magnetic skyrmions on a two-lane racetrack," New J. Phys. **19**(2), 025002 (2017).

[28] C. Abert, L. Exl, F. Bruckner, A. Drews, and D. Suess, "Magnum.fe: A micromagnetic finite-element simulation code based on FEniCS," J. Magn. Magn. Mater. **345**, 29–35 (2013).

[29] W. E. W. Ren and E. Vanden-Eijnden, "Simplified and improved string method for computing the minimum energy paths in barrier-crossing events," J. Chem. Phys. **126**(16), 164103 (2007).

[30] C. Moreau-Luchaire *et al.*, "Additive interfacial chiral interaction in multilayers for stabilization of small individual skyrmions at room temperature," Nat. Nanotechnol. **11**(5), 444–448 (2016).

[31] J. Sampaio, V. Cros, S. Rohart, A. Thiaville, and A. Fert, "Nucleation, stability and current-induced motion of isolated magnetic skyrmions in nanostructures," Nat. Nanotechnol. **8**(11), 839–844 (2013).

[32] A. Thiaville, S. Rohart, É. Jué, V. Cros, and A. Fert, "Dynamics of Dzyaloshinskii domain walls in ultrathin magnetic films," EPL Europhys. Lett. **100**(5), 57002 (2012).

[33] P. J. Jensen, "Rapid evaluation of oscillating lattice sums," Ann. Phys. **509**(4), 317–326 (1997).

[34] G. Ju *et al.*, "High density heat assisted magnetic recording media and advanced characterization—Progress and challenges," in Magnetics Conference (INTERMAG), 2015 IEEE, 2015, S. 1–1.

[35] S. Mittal, "A Survey of techniques for architecting processor components using domain-wall memory," J Emerg Technol Comput Syst **13**(2), 29:1–29:25 (2016).